Short Papers

A New Active Array Module for Spatial Power Combiners and Active Antennas

Ying Shen, Charles Laperle, Nagula Sangary, and John Litva

Abstract—**We present the design and performance of a new module of spatial power combiners, which consists of four symmetrical slot coupled patch radiators and four MESFET negative resistance elements, based on a single active antenna design. These circuits are suitable for use in millimeter-wave systems as well as at microwave frequencies. Tests carried out with a prototype circuit showed a radiated power of 20.44 mW with about 16% dc-to-RF efficiency at 8.7 GHz. Feed networks for linear polarization and circular polarization are discussed. Design procedures for dual-frequency application are also addressed.**

I. Introduction

In the literature, much evidence is found proving that active antennas have advantages, including electronic beam steering, fast adaptive beam forming/nulling, and multibeam operation. Furthermore, if distributed power amplifiers (transmit case) or low-noise amplifiers (receive case) are integrated with the radiating elements, losses illumination profile can be precisely controlled. Additional advantages of such active antennas include the fact that in the transmit case, a high output power can be achieved by space combining the outputs of many low-power solid-state sources, and that graceful degradation will occur if some of the solid-state devices should fail.

In many practical applications, it would be very useful to be able to combine the output powers of a large number of solid-state devices. Many approaches for RF power combining have been demonstrated in the microwave and millimeter-wave frequency range [1]–[3]. Classical power-combining schemes were developed using waveguide cavities [4], but they become impractical at millimeter-wave frequencies, since the waveguide dimensions become very small and losses in the metal walls are high. Mink [5] suggested combining a large number of devices in free space. Based on a single element active antenna design, this paper reports on a new circuit array structure in which four symmetrical MESFET's are integrated with four slot coupled patch antennas to form an FET-active power combiner.

For this configuration, multilayer slot coupled patch antennas were chosen because radiation from the feed line does not affect the antenna pattern, and the feed network need not be fabricated using the same substrate material as the antenna elements. FET's are chosen as active elements because they have higher efficiencies and lower noise figures than either IMPATT or Gunn diodes, and can be easily incorporated into monolithic structures. In addition, this structure does not require an external locking signal, and the power combining is done in free space.

Manuscript received Oct. 11, 1993; revised June 27, 1994.

Y. Shen is with Harris Farinon Canada, Inc., DDO, P.Q., H9B 3G4, Canada.
C. Laperle is with the Department of Electrical Engineering, Laval University, P.Q., G1K 7P4, Canada.
N. Sangary and J. Litva are with the Communications Research Laboratory, McMaster University, Hamilton, Ont., L8S 4K1, Canada.

IEEE Log Number 9407446.

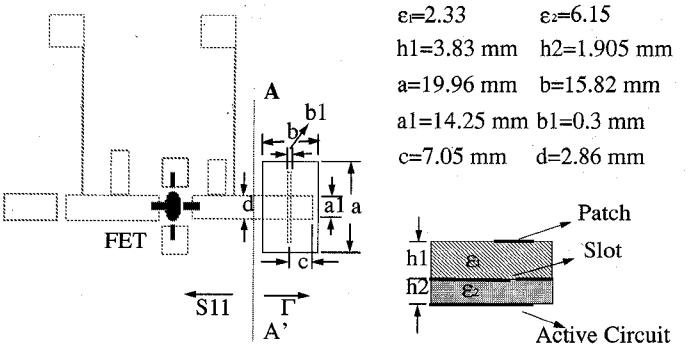

Fig. 1. The structure used for the active oscillator antenna.

II. Element Circuit Design

Whatever designs are used for active antennas, it is very important at the onset to carry out an accurate calculation for the input impedance of the antenna. In this paper, the antenna is a multilayer slot coupled patch. Because of the complexity of this structure, the Finite-Difference Time-Domain (FDTD) method is used to carry out the analysis [6]. The simulations are then confirmed using an HP8510B network analyzer which is calibrated using the Through-Reflect-Line (TRL) technique [7].

In order to demonstrate the technique, a multilayer slot coupled patch antenna, with dimensions shown in Fig. 1, has been developed at 4.9 GHz. The 3-dB passband was from 4.3 to 5.6 GHz, corresponding to a VSWR of approximately 3:1, and the gain of the antenna was 8.7 dB. FDTD simulation was used to calculate the reflection coefficient of the multilayer antenna. The simulation and experimental results were in good agreement [6].

After obtaining the correct input impedance of the antenna, the general design rules applicable to amplifiers or oscillators can be used for designing the active antenna circuits. In this paper, the active antenna, viewed as an oscillator, was designed as a "reflection amplifier" [8]. The microwave source for the circuit was an NE71 083 GaAs FET.

As shown in Fig. 1, along the reference AA', S_{11} and Γ must satisfy the oscillation conditions [8]. The quantities $1/S_{11}$ and Γ were measured using the HP8 510B, and they satisfied the two stability criteria for oscillators [8].

The output power of the active antenna was measured using a horn antenna located at one end of an anechoic chamber with the active antenna located at the other end. The output power of the active antenna was measured to be 4.81 mW at 4.9 GHz [8]. The sinusoidal output of the antenna was observed to be very stable with a clean spectrum. Fig. 2 shows the E- and H-plane field patterns for the active antenna.

III. Four-Element Active Array Antenna

Based on a single active antenna element design, a new array structure consisting of four symmetrical MESFET's integrated with four slot coupled patch antenna to form an FET-active antenna is now introduced.

An X-band prototype circuit has been developed to operate at 8.7 GHz. The array structure has one common gate and the distance between two opposite slots is 29.2 mm. The patch and the active

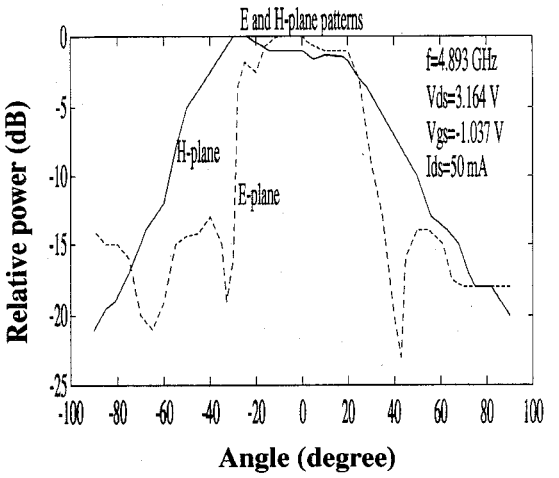

Fig. 2. E- and H-plane patterns of a one-element active antenna.

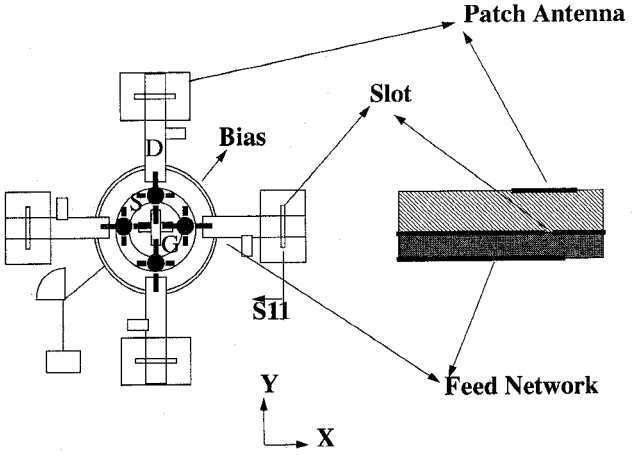

Fig. 3. Four-element active array structure.

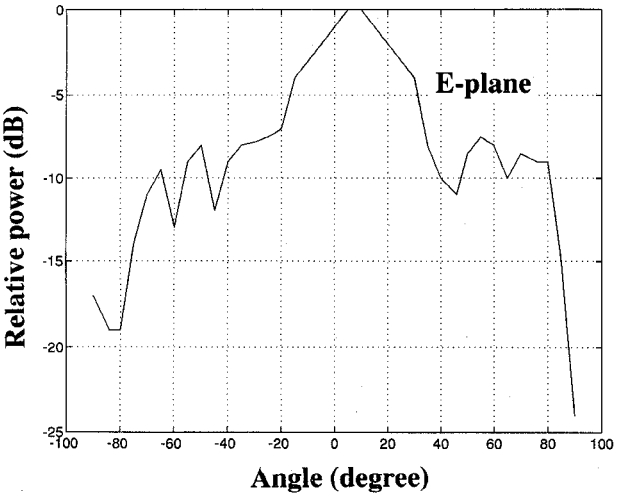

Fig. 4. Pattern of the four-element active antenna array.

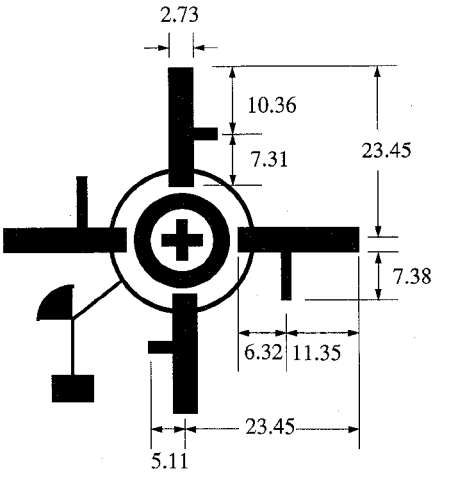

Fig. 5. Feed network for circular polarization.

circuit were fabricated on a 3.17-mm-thick Duroid 5880 substrate with $\epsilon_r = 2.33$ and a 1.905-mm-thick Duroid 6006 substrate with $\epsilon_r = 6.15$, respectively. The active elements were four NE76038 GaAs MESFET's. The array structure is shown in Fig. 3.

For the prototype circuit, the maximum output power is 20.44 mW at 8.7 GHz with about 16% dc–RF conversion efficiency. Fig. 4 gives the E-plane pattern for the active array. It is seen that the 3-dB beamwidth is approximately $\pm 15°$. The antenna was designed to be strong at 45° of the x-y direction. The measured axial ratio is greater than 30 dB. Frequency and power variations with bias of 100 MHz and 7 dB, respectively, were measured.

By changing the feed network, we were able to design a circularly polarized active antenna array. To achieve circular polarization with the four-element array, the signals fed to one pair of diagonally opposing elements remained unchanged, while the signals sent to the opposite pair were modified. The reflection coefficients at the slot coupling ports corresponding to the latter two patches were optimized to have the same amplitudes but to have phases which differ by 90°. Using the feed network shown in Fig. 5, we were able to develop a prototype antenna with an axial ratio < 2 dB.

IV. Dual-Frequency Application

We have found that if the feed network is further modified so that the opposing elements of the array are designed to operate at one frequency, and the other two are designed for another frequency, that a dual-frequency antenna can be achieved. EEsof's Touchstone software was used to optimize the performance of this antenna. Simulation results indicate two resonant frequencies—one at 8.7 and the other at 9.2 GHz. The reflection coefficients of the opposing elements of the array were designed to be the same at the two resonant frequencies. The phase at each slot was optimized to be the same. Tests on a prototype of this antenna showed good agreement between measurements and simulated results. Experimentally, it was found that the resonances occurred at 8.741 and 9.242 GHz.

V. Conclusion

A new module for an integrated active-array power combiner has been developed. The preliminary results show that this module has great potential for use in larger array systems and at higher frequencies. Further work is underway to investigate the application of this module in large arrays.

References

[1] Z. Y. Popovic, R. M. Weikle, II, K. A. Potter, and D. B. Rutledge, "Bar-grid oscillators," *IEEE Trans. Microwave Theory Tech.*, vol. 38, pp. 225–230, Mar. 1990.

[2] J. Birkeland and T. Itoh, "A 16 element quasioptical FET oscillator power combining array with external injection locking," *IEEE Trans. Microwave Theory Tech.*, vol. 40, pp. 475–481, Mar. 1992.

[3] J. Lin and T. Itoh, "Two-dimensional quasioptical power-combining arrays using strongly coupled oscillators," *IEEE Trans. Microwave Theory Tech.*, vol. 42, pp. 734–741, Apr. 1994.
[4] K. Kurokawa, "The single-cavity multiple-device oscillator," *IEEE Trans. Microwave Theory Tech.*, vol. MTT-19, pp. 793–801, Oct. 1971.
[5] J. W. Mink, "Quasioptical power combining of solid-state millimeter-wave sources," *IEEE Trans. Microwave Theory Tech.*, vol. MTT-34, pp. 273–279, Feb. 1986.
[6] J. Litva, Z. Bi, K. Wu, R. Fralich, and C. Wu, "Full-wave analysis of an assortment of printed antenna structures using the FDTD method," in *Proc. 1991 IEEE AP-S Int. Symp.*, June 1991, pp. 410–413.
[7] R. Fralich, J. Wang, and J. Litva, "Enhanced precision microstrip antenna measurements with nonstandard impedance lines at an arbitrary reference plane," McMaster Univ., CRL Rep. 228, Jan. 1991.
[8] Y. Shen, R. Fralich, C. Wu, and J. Litva, "Active radiating oscillator using a reflection amplifier module," *Electron. Lett.*, vol. 28, no. 11, pp. 991–992, May 1992.
[9] I. J. Bahl and P. Bhartia, *Microstrip Antennas*. Norwood, MA: Artech House, 1980.

A Single Barrier Varactor Quintupler at 170 GHz

Antti V. Räisänen, Timo J. Tolmunen, Mark Natzic, Margaret A. Frerking, Elliott Brown, Hans Grönqvist, and Svein M. Nilsen

***Abstract*— InGaAs/InAlAs single-barrier varactor (SBV) diodes are tested as frequency quintuplers. The diodes were tested in a crossed-waveguide structure and provided output frequencies between 148 and 187 GHz. The highest observed flange-to-flange efficiency was 0.78% at an output frequency of 172 GHz. This is nearly four times greater than the best quintupler efficiency obtained for previous SBV varactors made from the GaAs/AlGaAs materials system.**

I. Introduction

Harmonic multiplication of fundamental-frequency oscillators has long been a useful means of generating coherent power at frequencies above 100 GHz. A very effective device for harmonic multiplication has been the varactor diode, particularly the back-biased Schottky-barrier device [1]. Recently, interest has grown in novel varactor diodes having symmetric capacitance-versus-voltage (C-V) characteristic about zero bias. This property suppresses the generation of even harmonics, which simplifies the design of high-harmonic multipliers (e.g., quintuplers) because of the reduction in the number of idler circuits.

This paper concerns the single-barrier varactor (SBV) diode (also known as the quantum-barrier varactor [2], [3]). Theoretical analysis indicates that SBV diodes are good candidates for millimeter and submillimeter wave multipliers with predicted efficiencies as high as 18% at 1000 GHz [4]. In simplest form, the SBV diode consists of two n-type semiconductor cladding layers separated by an electron barrier layer. The doping profile in the cladding layers is perfectly symmetric about the center of the barrier so that the C-V characteristics is symmetric about zero bias. With cladding layers made of GaAs and the barrier of AlGaAs, SBV diodes have been demonstrated as triplers with output between 200 and 300 GHz, yielding a maximum flange-to-flange efficiency of 5% at 222 GHz [3] and 2% 192 GHz [5]. The SBV diode in Ref. 3 was also tested as a quintupler at 310 GHz, yielding a maximum efficiency of 0.2%.

In the present work, we examine SBV diodes made with InGaAs cladding layers and an InAlAs barrier. This combination of materials yields a larger barrier height with less excess conduction current compared to the GaAs/AlGaAs SBV diodes. Two different SBV diodes, one made at MIT Lincoln Laboratory and the other made at the Chalmers University of Technology, were tested in a waveguide quintupler structure with output between 148 and 187 GHz.

II. Multiplier Devices

Both the Lincoln and Chalmers diodes consisted of an $In_{0.53}Al_{0.47}As$ barrier embedded between n-type $In_{0.53}Ga_{0.47}As$ cladding layers. The epitaxial layers, depicted in Fig. 1, were grown by molecular beam epitaxy on an InP substrate. In order to assist the whisker contacting of mesa diodes, the regions between mesas in the Lincoln diode were filled with Si_3N_4 and via holes were opened to the SBV mesas by reactive ion etching. The same procedure was carried out on the Chalmers diode with photoresist instead of Si_3N_4. The Lincoln and Chalmers diodes have areas of about 16 μm^2 and 30 μm^2, respectively. Fig. 2 shows the measured I-V characteristics of the Lincoln device. Its zero-bias capacitance was 26 fF, as measured with a capacitance bridge at 1 MHz. Beyond ± 0.4 V, conduction current prevented capacitance measurements using the bridge. Fig. 3 shows the measured I-V and C-V characteristics of the Chalmers device. The leakage current of the Chalmers diode is considerably higher than that of the Lincoln diode. This is due to the high doping level of the barrier (see Fig. 1) which was applied in order to increase the C_{max}/C_{min} ratio. The C-V characteristic together with the series resistance was measured using a vector network analyzer between 50 MHz and 26.5 GHz [6]. The zero bias capacitance was 50 fF and the series resistance was typically between 8 and 9 Ω.

III. Quintupler Mount

The SBV diodes were mounted in a crossed-waveguide quintupler structure in which the input and output waveguides are separated by a low-pass coaxial filter. Fig. 4 shows a schematic diagram of the quintupler structure. Pump radiation between 30 and 38 GHz is coupled in through a half-height WR-22 waveguide and is impedance matched to the coaxial filter using two non-contacting sliding backshorts. The SBV diode is soldered to the far end of the filter pin and is located in the third-harmonic idler cavity. The idler cavity and the output waveguide are coupled through a transition in the waveguide width. The idler cavity is tuned by a non-contacting sliding backshort. The coupling to the output waveguide is controlled by an E-plane tuner with a contacting backshort located just past the waveguide transition. The reduced-height output waveguide tapers linearly to a standard-height WR-4 waveguide. The SBV diode is dc biased (optimum bias 0 V) through a whisker contact across the idler cavity and through the coaxial filter, which is electrically insulated from the waveguide structure by two macor insulation rings.

Manuscript received December 27, 1993; revised June 9, 1994. The Lincoln Laboratory portion of this work was sponsored by NASA through the Jet Propulsion Laboratory.

A. V. Räisänen and T. J. Tolmunen are with the Radio Laboratory, Helsinki University of Technology, FIN-02150, Espoo, Finland.
M. Natzic and M. A. Frerking are with the Jet Propulsion Laboratory, California Institute of Technology, Pasadena, CA 91109 USA.
E. Brown is with the Lincoln Laboratory, Massachusetts Institute of Technology, Lexington, MA 02173 USA.
H. Grönqvist and S. M. Nilsen are with the Department of Applied Electron Physics, Chalmers University of Technology, S-41296 Göteborg, Sweden.

IEEE Log Number 9407463.